원격탐사 및 현장관측을 통한 최근 북극 해빙두께 변화 분석

Assessment of recent changes of sea ice thickness in the Arctic Ocean using remotely sensed and in-situ observations

University of Alaska Fairbanks, International Arctic Research Center

Submission

To : Chief of Korea Polar Research Institute

This report is submitted as the final report of entrusted research "**Assessment of recent changes of sea ice thickness in the Arctic Ocean using remotely sensed and in-situ observations**" project.

2020.02.19

Person in charge of Entire Research: Dr. A. Pnyushkov

Name of Entrusted Organization: University of Alaska Fairbanks,
International Arctic Research Center

Entrusted Researcher in charge: Dr. A. Pnyushkov

Participating Entrusted Researchers:

Dr. A. Pnyushkov, University of Alaska Fairbanks
Dr. Hyun-cheol Kim, Korean Polar Research Institute

Summary

Assessment of recent changes of sea ice thickness in the Arctic Ocean using remotely sensed and in-situ observations"

This project is aimed at improving our understanding of recent (2013-17) sea ice changes in the Arctic Ocean, drawing on comprehensive datasets of *in-situ* and satellite-based observations of sea ice thicknesses, ice roughness, concentrations, and ice velocities, complemented by oceanographic measurements in the upper ocean.

During the project, we carefully processed the upward-looking sonar record collected at oceanographic mooring located at the northern slope of Severnaya Zemlya (82°05.98'N, 97°01.82'E). The mooring was equipped with ice sonar manufactured by ASL Environmental Sciences aimed at precise (with an average accuracy of ~5 cm) collection of information about sea ice draft with a very high (~20 s) temporal resolution. Following project *Objectives*, we have estimated statistical measures of differences between the CryoSat-2, SMOS, and ULS ice thicknesses to quantify potential mismatch between the remotely-sensed and in-situ measurements of ice thickness in the Eurasian Basin. Additionally, for the assessment of thermodynamic growth of sea ice in the region in response to seasonal variability of atmospheric forcing, we performed simulations with a one-dimensional convection/sea ice model to quantify the impact of atmospheric and ocean heat on seasonal variability and year-to-year changes of sea ice thickness in the eastern EB. The model utilized describes the temporal evolution of temperature, salinity, and depth of the winter mixed layer during the thermal and haline stages of winter convection driven by density instability and induced by water cooling and brine rejection. The oceanic heat fluxes to the bottom of the ice and their contribution to the rates of ice growth were estimated directly as a part of the model solution.

Utilizing an archive of modern ice observations from the mooring located at the slope of Severnaya Zemlya in the eastern EB, enable us to provide unique two-year time and spatial series of quality-controlled ice thicknesses. Based on this data set, we estimated major statistics (monthly, seasonal, and annual estimates of the mean, median, mode, standard deviation, extremes, and PDFs) of sea ice thickness in the Eurasian Basin accompanied by measures of year-to-year changes. The comparison of major statistical parameters shows that both satellite products (CS-2 and CS2/SMOS) substantially (up to 40 cm) overestimate sea ice thickness for the moderate and thick ice and cannot be used without bias correction. The collected 2013-15 ULS record suggests that the ridged ice dominates over the level ice at the continental slope of the *Chukchi Sea* in 2014-15. This dominance indicates an important role that ice dynamics play in the formation of sea ice cover in the Canadian Basin of the Arctic Ocean. The most often occurrence of the ridged ice was evident in spring when this ice type was observed over ~60% of time in comparison with ~34% for the level ice. However, the strongest relative contribution of ridging to ice thickness was usually evident for the thin ice (<1 m) at the beginning of ice formation (from October through December), when the relative difference between the mean and modal ice thicknesses may be as strong as 70%. We have performed an attempt to compare KOMPSAT-5 SAR backscatter data with the SMOS sea ice thickness variance estimated over bi-weekly intervals as a qualitative measure of the ice deformation at the site of B2 mooring in the Chukchi Sea. The comparison suggests a small (R^2=0.12±0.25) and statistically insignificant correlations between the ice thickness variance and the KOMPSAT-5 backscattering and does not allow at this stage to develop a robust statistical relationship.

Table of Contents

Introduction

Sea ice thickness is a fundamental climate state variable that provides a complex measure of changes in the high-latitude energy balance [*Lindsay and Schweiger*, 2015; *Kwok and Untersteiner*, 2013]. In the last decade, sea-ice cover in the Arctic Ocean has experienced dramatic changes in all components including thickness, extent, and volume [e.g., *Tilling et al.*, 2015, 2017]. *Kwok and Rothrock* [2009] used a combination of submarine and satellite records from the central Arctic Ocean to show a 1.75 m decrease in the mean winter ice thickness since 1980, and the highest rate of sea-ice thickness decline of 0.1–0.2 m/yr over the last five years of the record. The most pronounced sea-ice loss during the two record-breaking years of 2007 and 2012 occurred in the Canadian Basin; however, during recent years (e.g., 2014-16) a sea-ice decline in the eastern Eurasian Basin (EB) was also substantial and at least comparable to or even exceeding that of the western Arctic. While the ice extent in the eastern Eurasian Basin is reasonably well observed by satellites, the available satellite-based products for ice thickness are not well validated versus in-situ observations [*Lindsay and Schweiger*, 2015]; and thus, demonstrate a large uncertainty in the rates of ice thickness decline for this region.

The overarching ***goal*** of this project is to improve our understanding of recent (2013-17) sea ice changes in the Arctic Ocean, drawing on comprehensive datasets of *in-situ* and satellite-based observations of sea ice thicknesses, ice roughness, concentrations, and ice velocities, complemented by oceanographic measurements in the upper ocean.

1. Project goal and objectives

The primary project <u>*objectives*</u> were specified as follows:

O1: To quantify recent changes of sea ice thickness in the Eurasian Basin at time scales from seasons to years using available Upward Looking Sonar (ULS) records, Cryosat-2, and Soil Moisture and Ocean Salinity (SMOS) satellite observations.

O2: Using high-resolution KOMPSAT-5 Synthetic Aperture Radar (SAR) observations in the Chukchi Sea to provide the assessment of sea ice deformation and to quantify the contribution of dynamic pressure ridging to regional variations of sea ice.

O3: To validate estimates of Cryosat-2 and SMOS ice thicknesses for different seasons by comparison with Upward Looking Sonar observations collected in the Eurasian Basin of the Arctic Ocean, and to quantify biases between remotely-sensed and in-situ measurements of ice thicknesses.

2. ULS record processing at oceanographic mooring in the eastern Eurasian Basin

At the first stage of the project we carefully processed the ULS record collected at mooring M6 located at the northern slope of Severnaya Zemlya (82°05.98'N, 97°01.82'E, 2710 m depth; **Fig. 1**) – an essential step in meeting the project objectives. This mooring was deployed at the continental slopes of the Laptev Sea in the eastern part of the EB – the extensive area not covered yet with long-term in-situ observations of sea ice thickness. The mooring was equipped with an acoustic ice sonar (Upward-looking sonar; ULS) manufactured by ASL Environmental Sciences aimed at precise (with an average accuracy of ~5 cm) collection of information about sea ice draft with a very high (~20 s) temporal resolution.
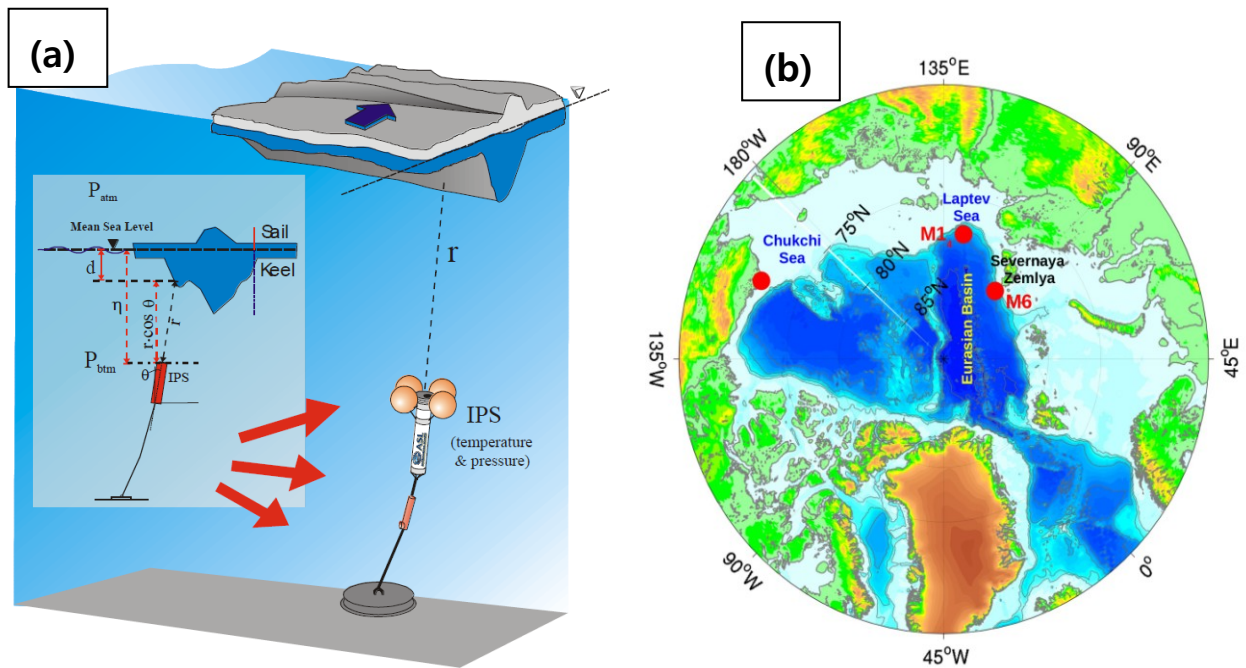
Figure 1. (a) Schematic of an acoustic Upper Looking Sonar utilized for measuring the sea ice draft. (b) Map showing locations of the moorings with Upward Looking Sonar records in the eastern Eurasian Basin of the Arctic Ocean and in the Chukchi Sea.

A routine of sonar signal processing is a very time-consuming task and takes up to three months for managing one annual record (processing of ~1.5M individual ice draft measurements). Ice sonar data processing was carried out employing the recent version of the ASL Environmental Sciences Processing Toolbox package (stand-alone application; version 1.2; February 2017), which was developed by the manufacturer of the ULS instruments. In the past, this package has been applied successfully for processing of numerous ULS data sets collected in different parts of the Arctic Ocean (e.g., *Melling and Riedel*, [2008]; *Chave et al.,* [2004]; *Hansen et al.,* [2015] and others).

In order to increase the accuracy of ice draft estimates retrieved from ULS acoustic signals, several important corrections were applied during data processing. For instance, we carried out correction of sound speed caused by changes of water density in the upper ocean layer, which serve as a major source of uncertainties for the ULS-derived ice thicknesses [*Melling et al.,* 1995]. For calculation of the speed of sound at moorings equipped with the ULS instruments we used temperature and salinity observations measured in the upper ocean. For the calculation of the speed of sound at the mooring we used temperature and salinity observations measured by a SBE-37 instrument in the upper ocean (**Fig. 2**). Following approach by *Pickart et al.* [2013], to fill gaps in temperature and salinity coverage in proximity to the ice base we extrapolated observations from the uppermost instrument upward to the rest of water column, assuming vertically-uniform distribution of temperature and salinity within this layer.

An additional correction of the ULS "pseudo" ice drafts was performed to take into account changes of atmospheric pressure at mooring positions, which affect the estimates of the instrument's depth derived from pressure sensor measurements. For this correction we used hourly output from the ERA-5 reanalysis model and interpolate the simulated sea-level pressure to the position of the mooring for the period covered by ULS measurements (i.e., from September 2013 through September 2015). Additional time series of air temperature,

wind speed, and ice concentration restored to the mooring position was used to identify and validate periods of open water – the essential step in the processing for referencing (estimates of zeros) acoustic ice drafts (see the *ULS Processing User's manual 2017*, for details).

The processing of the ULS data have shown that the ULS record at M6 moorings in 2013-15 has good quality and does not contain substantial data gaps (**Fig. 3**). All statistical estimates of ice drafts are accompanied by their confidence intervals to quantify uncertainties in our analysis using bootstrap method (see *Davison and Hinkley* [1997] for details). We used these intervals to evaluate potential uncertainties in our analysis of ice changes in the eastern EB and during the comparison with satellite ice thicknesses. Original high-resolution (20 seconds) time-series of the ULS ice thicknesses will be averaged over daily time intervals to reproduce highest resolution of raw Cryosat-2 and SMOS observations and will be used further for statistical analysis and comparison.
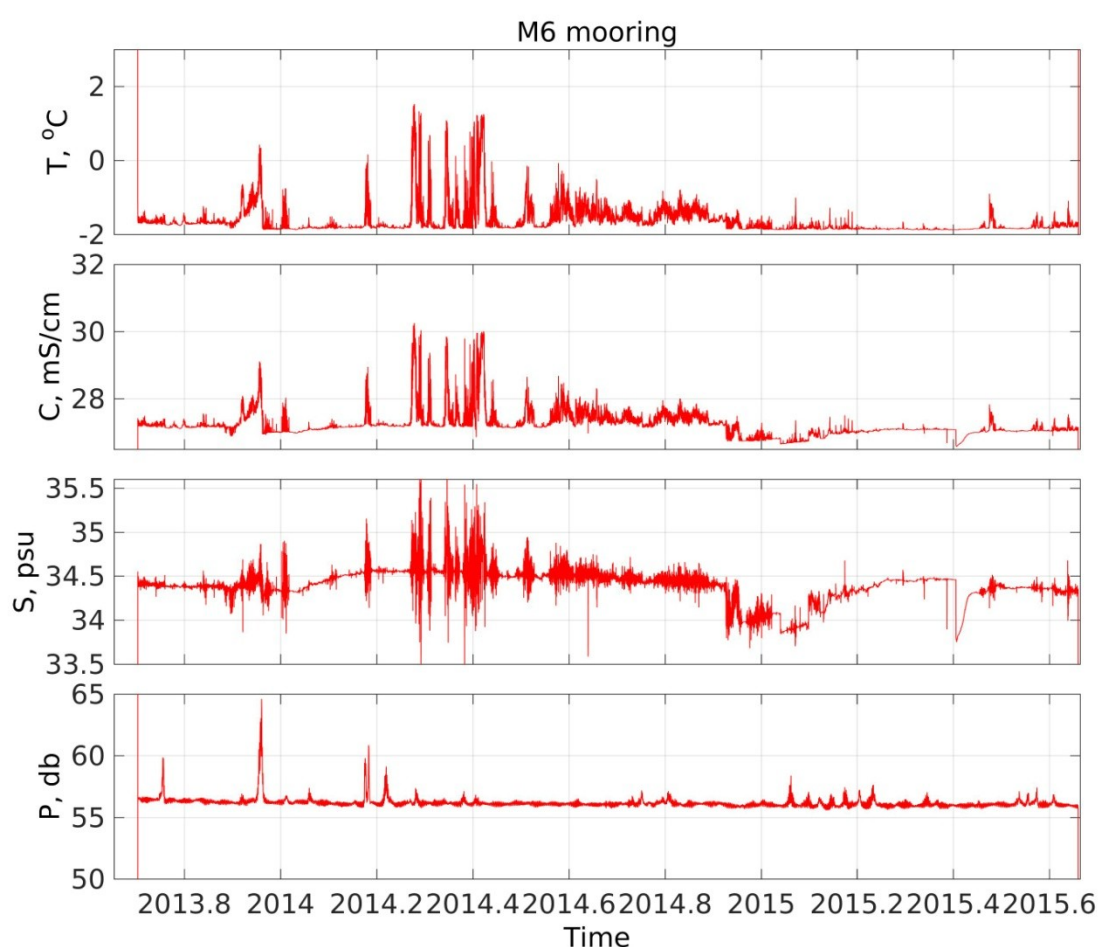

Figure 2. Time series of temperature (T), conductivity (C), salinity (S), and pressure (P) derived from a SBE-37 Microcat instrument deployed at the M6 mooring in 2013-15 by the Nansen and Amundsen Basins Observational System (NABOS) program.

At the final step of ULS data processing the original high-resolution (20 seconds) time-series of the ULS-derived ice thicknesses was averaged over daily time intervals to reproduce highest resolution of raw CryoSat-2 and SMOS observations used for statistical analysis and comparison. A spatial series of ice drafts was calculated from daily ice thickness record by

6

utilizing ice velocity measurements interpolated linearly to the site of M6 mooring and was compared with temporal series to assess the potential impact of variable speed of ice advection on the sea ice thickness distributions. For that task, we used daily Polar ice motion vectors available at an equally-spaced (with a 25-km resolution) EASE grid [*Tschudi et al.,* 2016]. The comparison in the probability distribution functions for the spatial and temporal ice thickness records shows insignificant difference among them, so that the solely temporal series of ice thickness may be used for the statistical evaluation of ice thickness at the Severnaya Zemlya slope.
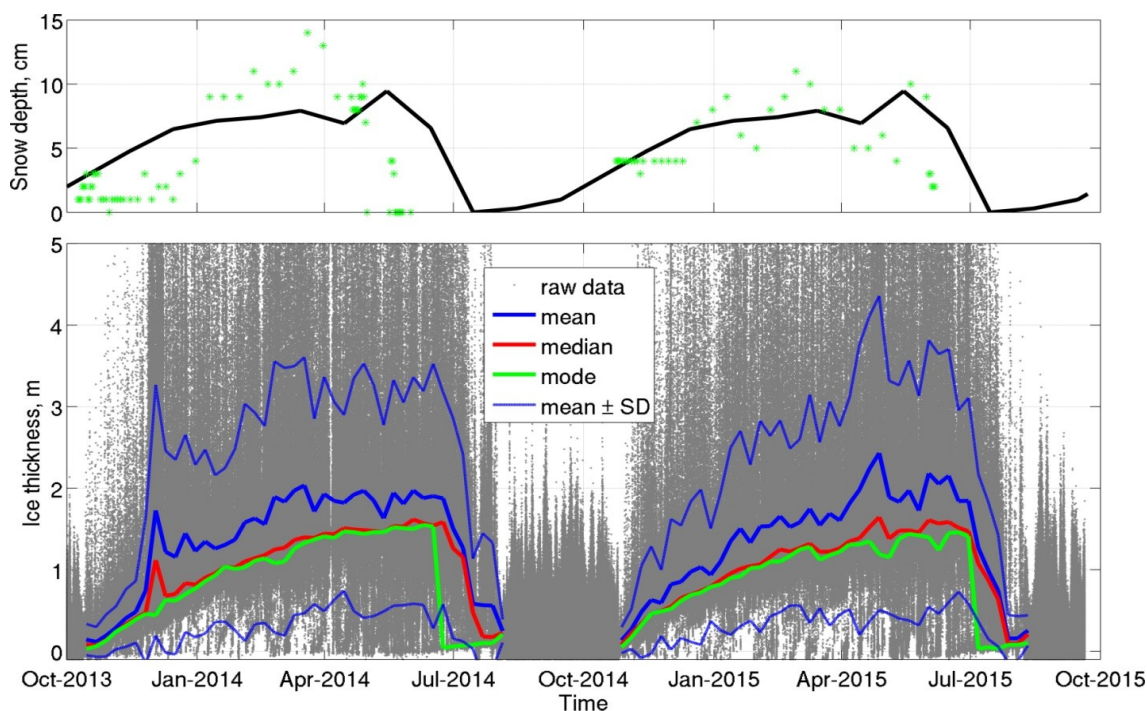

Figure 3. (Top) Environmental Working Group (EWG) climatological snow depth (cm) on surface of sea ice at the M6 mooring site at the Laptev Sea slope in 2013-15. Green stars show snow depths measured at the Tiksi meteorological station in 2013-15. (Lower panel) Sea ice thickness measured by the Ice Profiling Sonar at the M6 mooring in 2013-15 (grey dots).

Deliverables: *Utilizing an archive of modern ice observations from the mooring located at the slope of Severnaya Zemlya in the eastern EB, this project provides two-year time and spatial series of quality-controlled ice thicknesses, accompanied by their confidence intervals. Major statistics (monthly, seasonal, and annual estimates of the mean, median, mode, standard deviation, extremes, and PDFs) accompanied by measures of year-to-year changes.*

3. Comparison of CryoSat-2, SMOS, and ULS ice thicknesses

The processed 2013-15 series of sea ice thicknesses at the M6 mooring provides a unique opportunity for validation of satellite-based ice products for the region, where *in-situ* observations are rare due to harsh ice and weather conditions. Using spatial interpolation we have restored CS2 and SMOS ice thickness at the positions of the M6 mooring. Further, this series was used to calculate PDFs of ice thickness at the mooring site as well as major

statistical parameters (e.g., means, medians, modes, standard deviations) on a monthly, seasonal, and annual basis.

Following *Objective#1*, we have estimated biases and root-mean-squared differences between the Cryosat-2, SMOS, and ULS ice thicknesses to quantify potential mismatch between the remotely-sensed and in-situ measurements of ice thickness in the EB. We note that the satellite products like CryoSat-2 and merged CS-2/SMOS have very limited measurements of thin (<0.5 m) ice, thus the comparison of those data with ULS measurements at M6 and M1-4 moorings is not statistically robust. We have performed a separate comparison of ice thickness for the moderate (<1m) and thick (>1 m) ice periods of covered by ULS measurements to evaluate how properties of ice cover (surface emissivity, freeboard height, snow cover, etc.) may affect these differences. The comparison of major statistical parameters shows that both satellite products (CS-2 and CS2/SMOS) substantially (up to 40 cm) overestimate sea ice thickness for the moderate and thick ice and cannot be used without bias correction (**Fig. 3**). The young forms of ice evident at the site of M6 mooring from November through December are hardly detectable with those ice products. The deviations between those products for the thin ice, typically, were larger compared to thick ice (up to 50 cm) suggesting that an additional correction of satellite product should be applied for the Eurasian Basin to gain a better agreement with in-situ observations during the beginning of ice growth season.

For the assessment of thermodynamic growth of sea ice in response to seasonal variability of atmospheric forcing, we performed simulations with a one-dimensional convection/sea ice model to quantify the impact of atmospheric and ocean heat on seasonal variability and year-to-year changes of sea ice thickness in the eastern EB (*Objective #1*). For that, we utilized the convection model originally proposed by *Rudels et al.*, [1996], which was successfully implemented for the western EB by *Ivanov et al*. [2016]. The model describes the temporal evolution of temperature, salinity, and depth of the winter mixed layer during the thermal and haline stages of winter convection driven by density instability and induced by water cooling and brine rejection. The oceanic heat fluxes to the bottom of the ice and their contribution to the rates of ice growth were estimated directly as a part of the model solution. The model was forced with daily Era-Interim heat fluxes starting in the beginning of ice formation in the EB (in the mid-October) until the end of ice growth season, when the net heat fluxes become positive.

The estimates of ice thickness measured by the ULS at the M6 mooring were compared with those simulated in the convection/sea ice model (**Fig. 5**). The rates of winter sea ice growth estimated from the ULS records and simulated in the 1D convection model accompanied by the oceanic heat fluxes helps answering a more general question about the role of oceanic processes (e.g., winter convection, ventilation of halocline, etc.) in regional changes of sea ice state and validate the conception of "atlantification" of the eastern EB [*Polyakov et al.,* 2017].
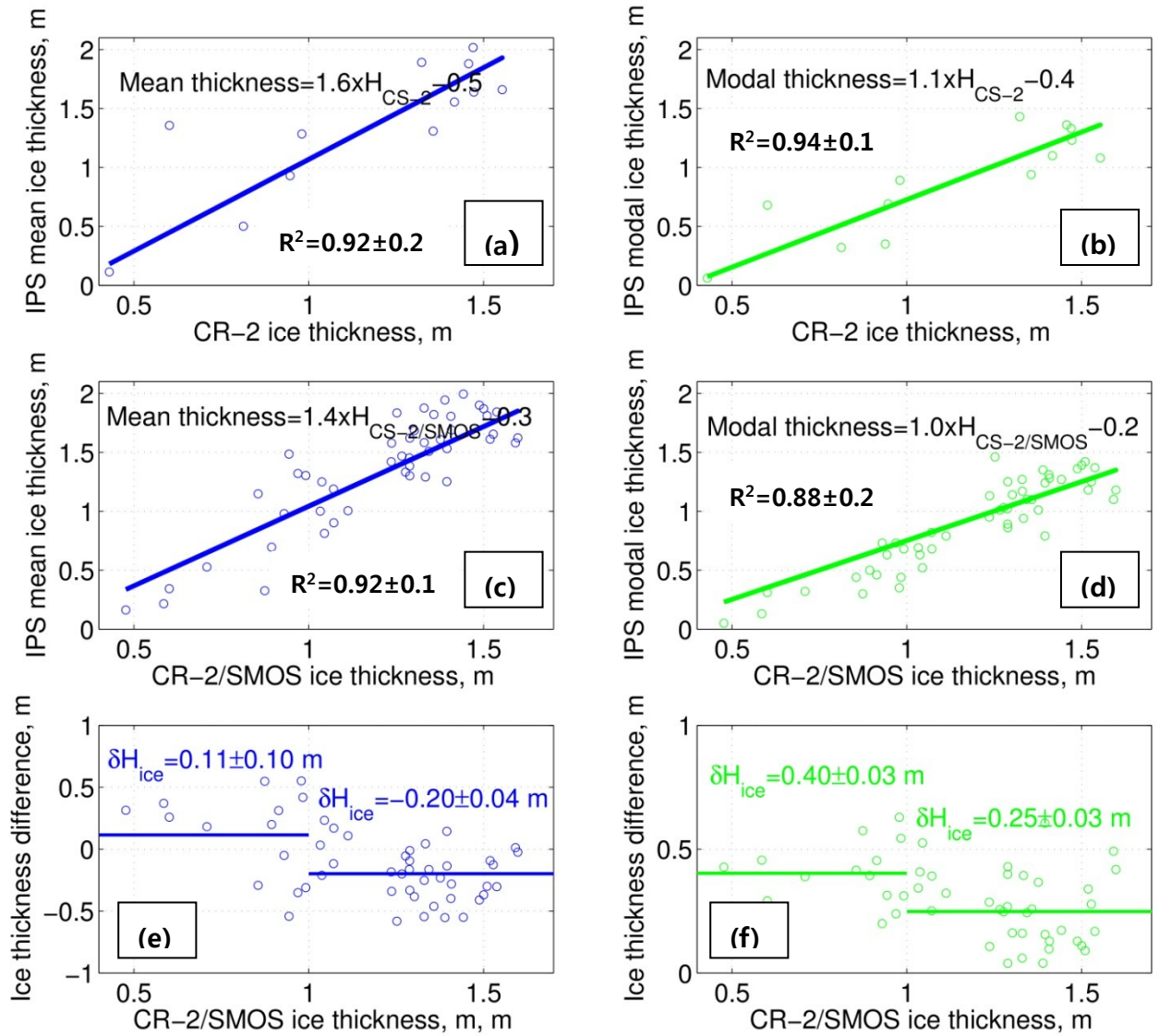
Figure 4: Relationship between the mean (a, c)/modal (b, d) ice thicknesses estimated using the 2013-15 ULS series at the M6 mooring site and from the CryoSat-2 and CryoSat-2/SMOS data sets. Panels (e) and (f) show bi-weekly differences (color circles) between the ULS-based mean/modal ice and CryoSat-2/SMOS thicknesses. Horizontal lines in (e)-(f) indicate mean differences for the thin (h<1 m) and thick (h>1m) ice types. Squared correlation coefficients (R^2) were calculated between the ULS- and satellite-based ice thickness records.
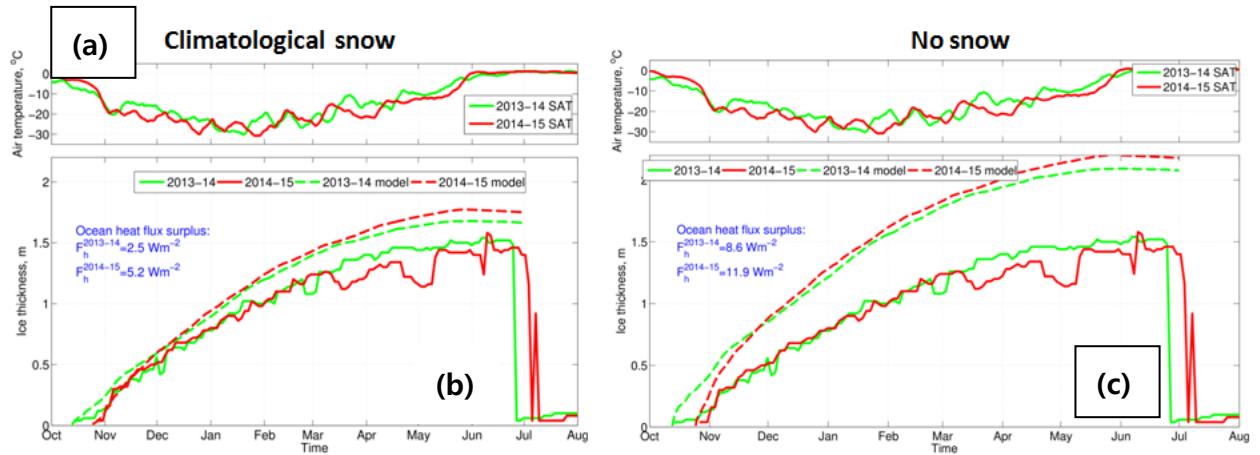
Figure 5. (a) Surface air temperature (SAT) derived from the Era-5 reanalysis model at the site of the NABOS M6 mooring in 2013-15. (b) Solid green and red series show modal sea ice thickness derived from the instrumental ULS observations at the M6 mooring. The simulated sea ice thickness during the ice growth season is shown by dashed lines. The simulated growth of sea ice was due to atmospheric forcing only (no heat fluxes from the ocean to the bottom of sea ice were applied). Thus, the differences in the simulated and measured ice thickness enable estimating the oceanic heat fluxes to the ice surface (blue numbers). (c) The same as in (b) but with no snow accumulation on top of sea ice.

Performed simulations suggest that the ocean warmth contributes to basal melting of sea ice through the net (over the ice growth season) heat flux surplus of an order of 5 Wm^{-2}. These estimates are comparable with the estimates of oceanic heat fluxes through the halocline layer estimated using the ocean heat content changes at moorings in the Eurasian Basin of the Arctic Ocean (e.g., Polyakov et al., [2013; 2017]).

Major deliverables: *Quality-controlled time-series and spatial maps of ice thicknesses for the Cryosat-2 and SMOS data set. Monthly estimates of the mean, modes, standard deviations, correlations, and PDFs for the Cryosat-2 and SMOS ice thicknesses; Statistical relationship between the mean and modal ice thicknesses estimated using the 2013-15 ULS record at the M6 mooring site and from the CryoSat-2 and CS-2/SMOS data sets. Estimates of biases between the ULS and CS-2 and CS2/SMOS ice products.*

4. Assessment of sea ice deformation in the Chukchi Sea using ULS and KOMPSAT-5 SAR data

We estimated impact of ice deformation on sea ice thickness at the B2 mooring site in the Chukchi Sea (71°12'N, 157°41'W) in 2014-15 by calculating separated monthly statistics for the level (undeformed) and ridged ice. For this separation, we used the criterion suggested by *Melling and Riedel [1995]* for the Beaufort Sea, in which the draft of level ice may vary by less than 0.25 m over ice segments of 10-m length. We note however, that the utilized criterion likely is not applicable for the summer months (June-August) because substantial pressure ridging in this period is very unlikely due to large areas of open water, so that the suggested criterion mostly represents natural heterogeneity of melted ice, but not ridging.

The calculated probability density functions of sea ice thickness for the level and ridged ice types is shown in **Fig. 5**. The collected 2013-15 ULS record suggests that the ridged ice dominates over the level ice at the continental slope of the Chukchi Sea in 2014-15. This dominance likely indicates an important role that ice dynamics plays in the formation of sea ice cover in the Canadian Basin of the Arctic Ocean. The most often occurrence of the ridged ice was evident in spring when this ice type was evident at ~60% of time in comparison with ~34% of the level ice. However, the strongest relative contribution of ridging to ice thickness was usually evident for the thin ice (<1 m) in the beginning of ice formation (from October through December), when the relative difference between the mean and modal ice thicknesses may be as strong as 70%.

We have performed an attempt to use KOMPSAT-5 SAR images alongside the ULS-based ice draft measurements in the coastal Chukchi Sea to provide insights into the sea ice deformation. For this task, we used the Chukchi Sea mooring site (71°12'N, 157°41'W) as a test polygon where we investigated the reliability of KOMPSAT-5 SAR imagery for use in the quantitative assessment of ice ridging and fracturing. The SAR images with a very high (~6 m) spatial resolution were collected for the position of Chukchi Sea mooring starting 10 October 2018, that prevent direct comparison of these data with ULS observations. Instead of direct ULS measurements, we used SMOS sea ice thickness variance estimated over bi-weekly intervals as a qualitative measure of the ice deformation at the site of mooring. However, small (R^2=0.12±0.25) and statistically insignificant correlations between the ice thickness variance and the KOMPSAT-5 backscattering does not allow at this stage to develop a robust statistical relationship.

__Deliverables__: Statistical properties of the level and ridged ice types estimated using the 2014-15 ULS record at the slope of the Chukchi Sea.
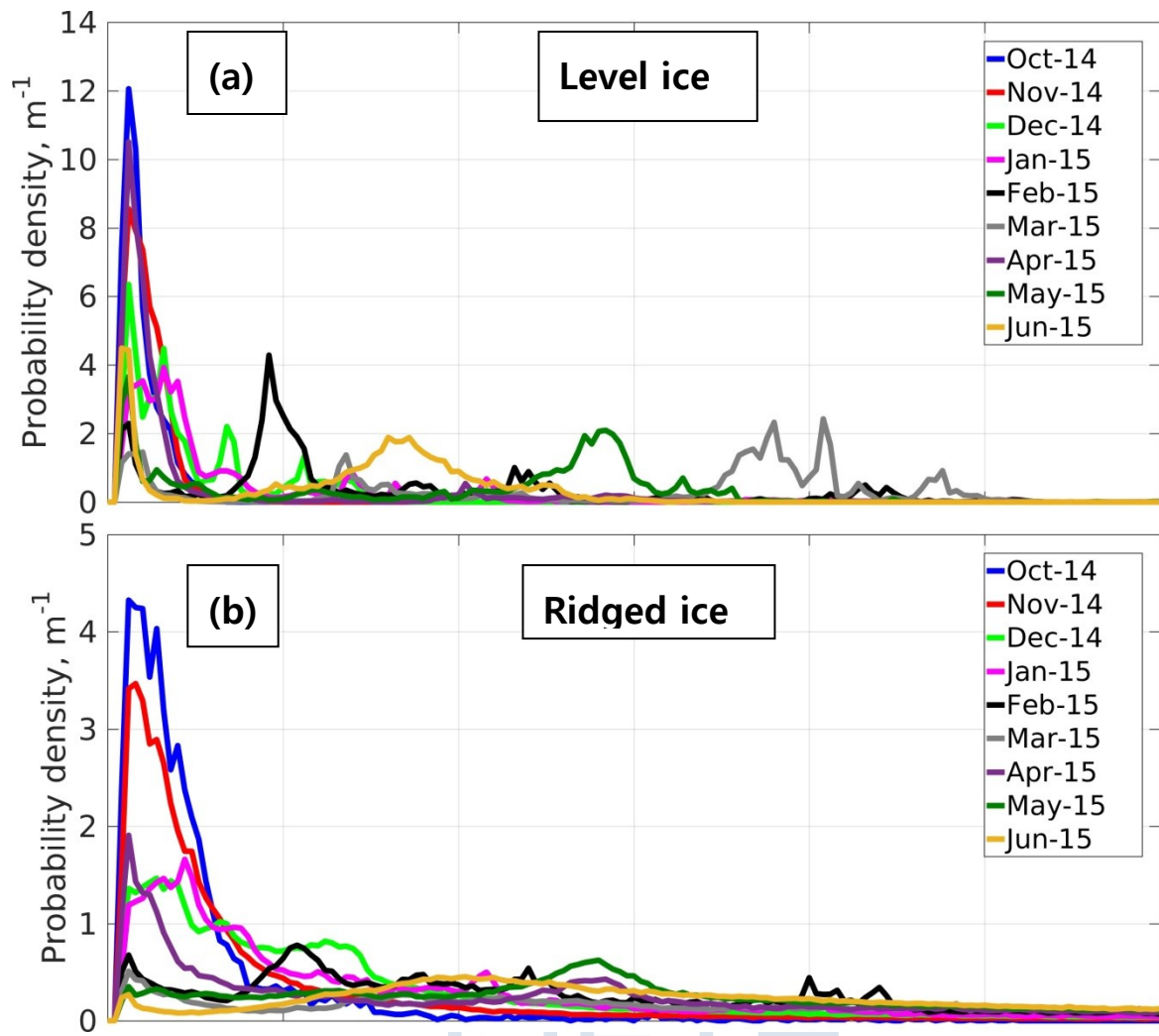
Figure 5. Probability density function of sea ice thickness for the level and ridged ice types at the B2 mooring in the Chukchi Sea in 2014-15.

***Outcome*:** A. Pnyushkov et al. (2018): Upward-looking sonar observations of ice thickness at the mooring over the Laptev Sea continental slope in the Arctic Ocean, *The Cryosphere*, paper in preparation.

References

Davison, A. C., and Hinkley, D. V., (1997): Bootstrap Methods and their Application. Cambridge University Press, Cambridge, 345 p.

Hendricks S., Ricker, R., Helm V., (2016): AWI CryoSat-2 Sea Ice Thickness Data Product (v1.2), User Guide., July 2016, available from http://data.meereisportal.de/data/cryosat2/doc/AWI_CryoSat2_Documentation_current.

Ivanov V, V. A. Alexeev, N. V. Koldunov, I. Repina, A. B. Sandø, L. H. Smedsrud, A. Smirnov, (2016): Arctic Ocean heat impact on regional ice decay – a suggested positive, Feedback, *J. Phys. Oceanogr.*, **46**, 1437–1456, doi:10.1175/JPO-D-15-0144.1.

Kwok, R., and D. A. Rothrock, (2009): Decline in Arctic sea ice thickness from submarine and ICESat records: 1958 – 2008, *Geophys. Res. Lett.,* 36, L15501, doi:10.1029/2009GL039035.

Kwok, R. and N. Untersteiner, (2011): The thinning of Arctic sea ice, *Physics today*, April 2011, 36-41.

Lindsay, R. and Schweiger, A., (2015): Arctic sea ice thickness loss determined using subsurface, aircraft, and satellite observations, *The Cryosphere*, **9**, 269-283, doi:10.5194/tc-9-269-2015,

Melling, H., P. H. Johnston, and D. A. Riedel, (1995): Measurement of the draft and topography of sea ice by moored subsea sonar, *J. Atmos. Oceanic Technol.*, **12**, 589-602.

Melling, H., D.A. Riedel, (2008): Ice Draft and Ice Velocity Data in the Beaufort Sea, 1990–2003, National Snow and Ice Data Center, Boulder, Colorado USA.

Pickart, R. S., Spall, M., A., and Mathis, J., T., (2013): Dynamics of upwelling in the Alaskan Beaufort Sea and associated shelf–basin fluxes, *Deep Sea Res., Part 1*, **76** (10), 35–51.

Polyakov, I.V., A.V. Pnyushkov, R. Rember, L. Padman, E.C. Carmack, and J.M. Jackson, (2013): Winter convection transports Atlantic water heat to the surface layer in the eastern Arctic Ocean, Journal of Physical Oceanography, **43**, 2142-2155.

Polyakov, I.V., Pnyushkov, A., Alkire, M., Ashik, I., Baumann, T., Carmack, E., Goszczko, I., Guthrie, J., Ivanov, V., Kanzow, T., Krishfield, R., Kwok, R., Sundfjord, A., Morison, J., Rember, R., Yulin, A., (2017) Greater role for Atlantic inflows on sea-ice loss in the Eurasian Basin of the Arctic Ocean. *Science*, **356**(6335), 285-291, doi:10.1126/science.aai8204.

Rudels, B., Anderson, L.G., Jones, E.P., (1996): Formation and evolution of the surface mixed layer and halocline of the Arctic Ocean. *J. Geophys. Res*., **101**, 8807-8821.

Tilling, R.L., Ridout, A., Shepherd, A., & Wingham D., J., (2015): Increased Arctic sea ice volume after anomalously low melting in 2013. *Nature Geoscience*, **8**, 643–646, doi:10.1038/ngeo2489.

Tschudi, M., Fowler, C., Maslanik, J., Stewart, J., S., and Meier, W., (2016): Polar Pathfinder Daily 25 km EASE-Grid Sea Ice Motion Vectors. Version 3. Boulder, Colorado USA: National Snow and Ice Data Center. doi: http://dx.doi.org/10.5067/O57VAIT2AYYY.

Warning

1. This report is a report of research results of a project entrusted by the Korea Polar Research Institute.

2. When you present the contents of this report, you must state that these contents are research results of a project entrusted by the Korea Polar Research Institute.

3. Materials concerning the nation's classified science and technology information must not be presented or disclosed.